Rare Event Simulation in Finite-Infinite Dimensional Space

Siu-Kui Au[1] and Edoardo Patelli[2]
Institute for Risk and Uncertainty
University of Liverpool, United Kingdom

Abstract

Modern engineering systems are becoming increasingly complex. Assessing their risk by simulation is intimately related to the efficient generation of rare failure events. Subset Simulation is an advanced Monte Carlo method for risk assessment and it has been applied in different disciplines. Pivotal to its success is the efficient generation of conditional failure samples, which is generally non-trivial. Conventionally an independent-component Markov Chain Monte Carlo (MCMC) algorithm is used, which is applicable to high dimensional problems (i.e., a large number of random variables) without suffering from 'curse of dimension'. Experience suggests that the algorithm may perform even better for high dimensional problems. Motivated by this, for any given problem we construct an equivalent problem where each random variable is represented by an arbitrary (hence possibly infinite) number of 'hidden' variables. We study analytically the limiting behavior of the algorithm as the number of hidden variables increases indefinitely. This leads to a new algorithm that is more generic and offers greater flexibility and control. It coincides with an algorithm recently suggested by independent researchers, where a joint Gaussian distribution is imposed between the current sample and the candidate. The present work provides theoretical reasoning and insights into the algorithm.

Keywords: Curse of dimension, Rare Event, Markov Chain Monte Carlo, Monte Carlo, Subset Simulation

1. Introduction

Modern engineering systems are designed with increasing complexity and expectation of reliable performance. Rare failure events with high consequences are becoming more

[1] Corresponding author. Harrison Hughes Building, Brownlow Hill, Liverpool, L69 3GH, UK. Email: siukuiau@liverpool.ac.uk.
[2] E-mail: Edoardo.patelli@liverpool.ac.uk

relevant to risk assessment and management. Unfortunately they are usually not well-understood and can even be out of imagination based on typical experience [1][2][3]. Studying failure scenarios allows one to gain insights into their cause and consequence, providing information for effective mitigation, contingency planning and improving system resilience. The probability and the consequence of failure events are two basic ingredients for trading off cost and benefit in the design of engineering systems. Assessing risk quantitatively requires proper modelling of the 'input' uncertain parameters by random variables as well as the logical/physical mechanism that predicts the 'output' quantities of interest. While no mathematical model is perfect, useful information can be gained if it is calibrated and interpreted properly, allowing one to make risk-informed decisions.

Let $\mathbf{X} = [X_1, ..., X_n]$ be the set of uncertain parameters in the problem, which are modeled by random variables. Without loss of generality $\{X_i\}_{i=1}^n$ are assumed to be standard Gaussian (zero mean and unit variance) and i.i.d. (independent and identically distributed). Dependent non-Gaussian random variables can be constructed from Gaussian ones by proper transformation [4]. One important problem in risk assessment is the determination of the failure probability $P(F)$ for a specified failure event F, which can be formulated as an n-dimensional integral or an expectation:

$$P(F) = \int I(\mathbf{x} \in F)\phi(\mathbf{x})d\mathbf{x} = E[I(\mathbf{X} \in F)] \tag{1}$$

where $I(\cdot)$ is the indicator function, equal to 1 if its argument is true and zero otherwise;

$$\phi(\mathbf{x}) = (2\pi)^{-n/2} \exp(-\frac{1}{2}\sum_{i=1}^{n} x_i^2) \qquad \mathbf{x} = [x_1, ..., x_n]^T \tag{2}$$

is the n-dimensional standard Gaussian PDF.

Monte Carlo methods [5][6][7] provide a robust means for risk assessment of complex systems. Problems of practical significance currently pose three main challenges: small probability, 'high dimension' (i.e., a large number of input random variables) and high complexity (e.g., nonlinearity) in the input-output relationship [8][9]. Small probability renders Monte Carlo method in its direct form computationally expensive or prohibitive. High dimension renders geometric intuitions in low dimensional space inapplicable or misleading [10][11]. High complexity means that the input-output relationship is only implicitly known as a 'black-box'.

1.1. Subset Simulation

Advanced Monte Carlo methods generally aim at reducing the variance of estimators beyond direct Monte Carlo method but in doing so they lose application robustness. Subset Simulation is a method that is found to play a balance between efficiency and robustness [12][13][14][15]. It has been applied to different disciplines and used for developing algorithms for related problems such as sensitivity [16][17][18] and design optimization problems [19][20][21][22][23][24]. There are variants that take advantage of prior knowledge of the problem, e.g., casual dynamical systems [25], transition from linear to nonlinear failure [26], meta-model [27]; or leverage on other computational tools, e.g., delayed rejection [28], Kriging [29] and neural networks [30].

Subset Simulation is based on the idea that a small failure probability can be expressed as the product of larger conditional probabilities of intermediate failure events, thereby potentially converting a rare event simulation problem into a sequence of more frequent ones. A general failure event is represented as $F = \{Y > b\}$, where Y is a suitably defined 'driving response' characterizing failure. In the actual implementation, Subset Simulation produces estimates for the values of b that correspond to fixed failure probabilities, from large to small values. The estimates make use of samples that populate gradually from the frequent to rare failure regions, corresponding to increasing threshold values that are adaptively generated.

A typical Subset Simulation run starts with 'simulation level' 0, where N samples of $\mathbf{X}$ are generated according to the parameter PDF $\phi(\mathbf{x})$, i.e., direct Monte Carlo. The values of the response Y are then calculated and sorted. The $p_0 N + 1$ largest value is taken as the threshold level b_1 for simulation level 1, where p_0 is the 'level probability' chosen by the user (conventional choice is 0.1). The top $p_0 N$ samples of $\mathbf{X}$ are used as seeds for generating additional samples conditional on $Y > b_1$, to make up a population of N conditional samples at level 1. The $p_0 N + 1$ largest value of Y among these samples is taken as the threshold level b_2 for simulation level 2. Samples for level 2 are generated and the procedure is repeated for higher threshold levels until the level of interest is covered.

1.2. Generation of conditional samples

The efficient generation of conditional failure samples, i.e., samples that are conditional on intermediate failure events, is pivotal to Subset Simulation. This is conventionally performed using an independent-component Markov Chain Monte Carlo (MCMC) algorithm [12][31][7], which is applicable for high dimensional problems and makes the algorithm robust to applications. For each X_i, let $p_i^*(\cdot;\cdot)$ be the proposal PDF assumed to be symmetric, i.e., Metropolis random walk. Suppose we are given a sample $\mathbf{X}^{(1)} = [X_1^{(1)},..., X_n^{(1)}]$ distributed as the target conditional distribution, i.e.,

$$\phi(\mathbf{x} \mid F) = P(F)^{-1} I(x \in F)\phi(\mathbf{x}) \tag{3}$$

According to the algorithm the next sample $\mathbf{X}^{(2)} = [X_1^{(2)},..., X_n^{(2)}]$ that is also distributed as $\phi(\mathbf{x} \mid F)$ is generated as follow:

Algorithm I (independent-component MCMC)

Step I. Generate $\mathbf{X}' = \{X_i'\}_{i=1}^n$

For $i = 1,..., n$

1. Generate ξ_i from the proposal PDF $p_i^*(\cdot; X_i^{(1)})$ and U_i uniformly on [0,1].

2. Calculate $r_i = \phi(\xi_i) / \phi(X_i^{(1)})$.

Set $X_i' = \xi_i$ if $U_i \le r_i$. Otherwise set $X_i' = X_i^{(1)}$.

End i

Step II (Check failure)

Set $\mathbf{X}^{(2)} = \mathbf{X}'$ if $\mathbf{X}' \in F$ (accept). Otherwise set $\mathbf{X}^{(2)} = \mathbf{X}^{(1)}$ (reject).

In the above, $\phi(x) = (2\pi)^{-1/2} \exp(-x^2/2)$ denotes the one-dimensional standard Gaussian PDF. The correlation among the conditional samples is an important factor influencing the efficiency of Subset Simulation. It is high (hence low efficiency) if $\mathbf{X}'$ is rejected too often in either Step I (MCMC mechanism) or Step II (not lying in the failure region); or when $\{\xi_i\}_{i=1}^n$ is of close proximity to $\mathbf{X}$ (governed by the proposal PDF).

1.3. Objectives and key findings

Theoretical arguments and numerical experience reveal that as the number of variables increases the rejection of the candidate $\mathbf{X}'$ tends to be governing by Step II; the efficiency of Subset Simulation is insensitive to the type of proposal PDF and may even be higher [12][15]. Motivated by this, for any given problem (generally finite dimensional) we consider an equivalent problem with an arbitrary number of random variables and investigate the limiting behavior of the algorithm as the number increases indefinitely. Specifically, each Gaussian variable X_i can be represented by an arbitrary (hence possibly infinite) number of 'hidden' Gaussian variables. As the key result of this work, we show that applying Algorithm I to the equivalent problem results in the following 'limiting algorithm' as the number of hidden variables is infinite:

Algorithm II (Limiting algorithm)

Step I. Generate $\mathbf{X}' = \{X_i'\}_{i=1}^n$

Generate $\mathbf{X}' = [X_1', ..., X_n']$ as a Gaussian vector with independent components, with mean vector $[a_1 X_n^{(1)}, ..., a_n X_n^{(1)}]$ and variances $[s_1^2, ..., s_n^2]$.

Step II (Check failure)

Set $\mathbf{X}^{(2)} = \mathbf{X}'$ if $\mathbf{X}' \in F$ (accept). Otherwise set $\mathbf{X}^{(2)} = \mathbf{X}^{(1)}$ (reject).

Algorithm II differs from Algorithm I only in Step I. Here, $0 \le s_i \le 1$ is the standard deviation of the candidate X_i' from the current sample and $a_i = \sqrt{1 - s_i^2}$. It is related to the proposal PDF but which is no longer relevant because the algorithm is now controlled directly through $\{a_i\}_{i=1}^n$ or equivalently $\{s_i\}_{i=1}^n$. This algorithm is remarkably simple and MCMC rejection no longer appears explicitly. As the algorithm does not depend on any details of the hidden variables, the infinite-dimensional equivalent problem is only involved at a conceptual level to arrive at the limiting result.

The limiting algorithm shows that it is possible to generate the candidate in Step I simply as a Gaussian vector whose statistics depend on the current sample. In fact the same algorithm has been recently proposed by independent researchers [32] who

ingeniously imposed this condition and verified this possibility. The present work provides a theoretical reasoning leading to the algorithm via a completely different route.

This paper is organized as follow. We first describe in Section 2 the equivalent problem with hidden variables that links the original problem and the conceptual infinite-dimensional problem. For ease of reading, the limiting behavior of the candidate and hence the MCMC algorithm is summarized in Section 3. Examples are then given in Section 4 to illustrate the results. The remaining sections provide the derivations for the limiting behavior and the results in Section 3.

2. Equivalent problem with hidden variables

Consider the reliability problem in the last section, where the number of random variables n need not be large. The original finite-dimensional problem can be represented by an equivalent problem with an arbitrary (hence possibly infinite) number of random variables as follow. First, each standard Gaussian X_i can be represented by n' i.i.d. standard Gaussian variables $\{Z_{ij}\}_{j=1}^{n'}$:

$$X_i = \frac{1}{\sqrt{n'}} \sum_{j=1}^{n'} Z_{ij} \tag{4}$$

This follows directly from the fact that 1) any linear combination of Gaussian variables is also Gaussian; and 2) the RHS of (4) has zero mean and unit variance. The total number of random variables in the problem is now $n'n$. Clearly, $n' \geq 1$ but is otherwise arbitrary. The representation in (4) is not unique but it is the one studied in this work. The set of random variables in the equivalent problem is

$$\mathbf{Z} = \{Z_{ij} : i = 1,...,n; j = 1,...,n'\} \tag{5}$$

instead of $\mathbf{X} = \{X_i\}_{i=1}^{n}$. These two sets of variables are related by a linear transformation, $\mathbf{X} = \mathbf{L}\mathbf{Z}$, whose form is not important and is omitted here. The response in the original problem depends on $\mathbf{X}$ and not directly on $\mathbf{Z}$. For this reason $\mathbf{Z}$ is called the set of 'hidden variables'.

2.1. MCMC algorithm applied to equivalent problem

Consider now applying the independent-component MCMC algorithm (Algorithm I) to the equivalent problem. Let $\mathbf{Z} = \{Z_{ij} : i = 1,...,n; j = 1,...,n'\}$ be the current conditional sample and $\mathbf{X} = \mathbf{L}\mathbf{Z} = \{X_i\}_{i=1}^{n}$. For each i, the one-dimensional proposal PDF for Z_{ij} is assumed to be symmetric and the same for different j. Without loss of generality it is denoted through the one-argument function $p_i^*(z)$, which is symmetric about 0. That is, if the i-th component of the current sample is z_i, then the candidate ξ_i is distributed as $p_i^*(\xi_i - z_i)$. In the above context, the MCMC algorithm for generating the next conditional sample given the current conditional sample $\mathbf{Z}$ reads as follow:

Algorithm I applied to equivalent problem with hidden variables

Step I. Generate $\mathbf{Z}' = \{Z'_{ij} : i = 1,...,n; j = 1,...,n'\}$

For $i = 1,...,n$

For $j = 1,...,n'$

1. Generate ξ_{ij} from the proposal PDF $p_i^*(\xi_{ij} - Z_{ij})$ and U_{ij} uniformly on [0,1].

2. Calculate $r_{ij} = \phi(\xi_{ij}) / \phi(Z_{ij})$.

Set $Z'_{ij} = \xi_{ij}$ if $U_{ij} \le r_{ij}$. Otherwise set $Z'_{ij} = Z_{ij}$.

End j

Set $X'_i = \frac{1}{\sqrt{n'}} \sum_{j=1}^{n'} Z'_{ij}$

End i

$\mathbf{X}' = [X'_1,..., X'_n]^T$

Step II (Check failure)

Set the next sample equal to $\mathbf{Z}'$ if $\mathbf{X}' \in F$ (accept). Otherwise set the next sample equal to $\mathbf{Z}$ (reject).

In the above algorithm we have deliberately avoided the symbol for the next sample (in Step II) to simplify notations. Although MCMC in Step I is performed in the $\mathbf{Z}$-space, it is the value of $\mathbf{X}$ that directly determines failure in Step II. For given $\mathbf{X}$, we shall

study the limiting distribution of $\mathbf{X}'$ in Step I when $n' \to \infty$. That is, we shall determine the following conditional PDF in the limit:

$$p_{\mathbf{X}'|\mathbf{X}}(\mathbf{x}' \mid \mathbf{x}) = p_{X_1',...,X_n'|X_1,...,X_n}(x_1',...,x_n' \mid x_1,...,x_n) \tag{6}$$

where $\mathbf{x}' = [x_1',...,x_n']$ and $\mathbf{x} = [x_1,...,x_n]$. Given $\mathbf{X} = [X_1,...,X_n]$, $\{X_i' : i = 1,...,n\}$ are generated independent of each other because $\{Z_{ij}'\}_{j=1}^{n'}$ for different i are generated independently in the inner loop. This means that

$$p_{\mathbf{X}'|\mathbf{X}}(\mathbf{x}' \mid \mathbf{x}) = \prod_{i=1}^{n} p_{X_i'|X_i}(x_i' \mid x_i) \tag{7}$$

It is therefore sufficient to study the one-dimensional conditional PDF $p_{X_i'|X_i}(x_i' \mid x_i)$.

3. Limiting distribution of candidate

For ease of reading we summarize in this section the analysis results for the conditional PDF of $\mathbf{X}' = [X_1',...,X_n']$ (associated with the candidate $\mathbf{Z}'$) given $\mathbf{X} = [X_1,...,X_n]$ (associated with the current sample $\mathbf{Z}$) in the algorithm in Section 2.1. By symmetry of the roles of X_i in Step I, it is clear that the result is identical for every $i = 1,...,n$. It can be shown that as $n' \to \infty$, conditional on $X_i = x_i$, X_i' has a Gaussian distribution with mean ax_i and variance s_i^2. That is,

$$p_{X_i'|X_i}(x_i' \mid x_i) = \frac{1}{\sqrt{2\pi}s_i} \exp[-\frac{1}{2s_i^2}(x_i' - a_i x_i)^2] \qquad n' \to \infty \tag{8}$$

where

$$a_i = 1 - 2\kappa_i \tag{9}$$

$$s_i^2 = 4\kappa_i - 4\kappa_i^2 \tag{10}$$

$$\kappa_i = \int_0^\infty w^2 \Phi(-\frac{w}{2}) p_i^*(w) dw \tag{11}$$

depends only on the proposal PDF p_i^*; $\Phi(\cdot)$ is the standard Gaussian CDF (cumulative distribution function). It can be shown that

$$0 \le \kappa_i \le 1 \qquad -1 \le a_i \le 1 \qquad 0 \le s_i \le 1 \qquad a_i^2 + s_i^2 = 1 \tag{12}$$

Remarkably, the limiting form of the conditional PDF that governs the transition of X_i does not depend on any detail about the hidden variables $\{Z_{ij}\}_{j=1}^{n'}$. In addition, it

satisfies the detailed balance condition with the standard Gaussian PDF $\phi(\cdot)$ as its stationary PDF:

$$p_{X_i'|X_i}(x_i' \mid x_i)\phi(x_i) = p_{X_i'|X_i}(x_i \mid x_i')\phi(x_i') \tag{13}$$

This implies that in the actual simulation one can directly generate the samples of $\mathbf{X}$ without the hidden variables. The latter serve only as a conceptual vehicle to arrive at the limiting result.

3.1. Justification for Algorithm II

Equation (13) can be used to show directly that the limiting algorithm presented in Section 1 indeed satisfies detailed balance in the presence of the conditioning from failure by exactly the same argument in [12]. That is, for all $\mathbf{x}^{(1)}$ and $\mathbf{x}^{(2)}$,

$$p_{\mathbf{X}^{(2)}|\mathbf{X}^{(1)}}(\mathbf{x}^{(2)} \mid \mathbf{x}^{(1)})\phi(\mathbf{x}^{(1)} \mid F) = p_{\mathbf{X}^{(2)}|\mathbf{X}^{(1)}}(\mathbf{x}^{(1)} \mid \mathbf{x}^{(2)})\phi(\mathbf{x}^{(2)} \mid F) \tag{14}$$

where $\phi(\mathbf{x} \mid F) = \phi(\mathbf{x})I(\mathbf{x} \in F)/P(F)$ denotes the standard Gaussian PDF conditional on failure. Essentially, Step II ensures that all samples along the Markov chain lie in the failure region and so it suffices to check detailed balance for only those states within the failure region, i.e., for all $\mathbf{x}^{(1)}, \mathbf{x}^{(2)} \in F$,

$$p_{\mathbf{X}^{(2)}|\mathbf{X}^{(1)}}(\mathbf{x}^{(2)} \mid \mathbf{x}^{(1)})\phi(\mathbf{x}^{(1)}) = p_{\mathbf{X}^{(2)}|\mathbf{X}^{(1)}}(\mathbf{x}^{(1)} \mid \mathbf{x}^{(2)})\phi(\mathbf{x}^{(2)}) \tag{15}$$

where $\phi(\cdot \mid F)$ has been replaced by $\phi(\cdot)$ because in this case both $I(\mathbf{x}^{(1)} \in F)$ and $I(\mathbf{x}^{(2)} \in F)$ are equal to 1. Thus, considering only the states in the failure region, detailed balance does not involve the conditioning from failure. Equation (15) holds trivially for $\mathbf{x}^{(1)} = \mathbf{x}^{(2)}$ and so it remains to consider $\mathbf{x}^{(1)} \neq \mathbf{x}^{(2)}$. In this case $\mathbf{X}^{(2)}$ must be equal to $\mathbf{X}'$ generated in Step I. The transition PDF $p_{\mathbf{X}^{(2)}|\mathbf{X}^{(1)}}(\cdot \mid \cdot)$ is then equal to the conditional PDF $p_{\mathbf{X}'|\mathbf{X}}(\cdot \mid \cdot)$ in (7). The latter satisfies detailed balance because its component counterpart in (13) does:

$$p_{\mathbf{X}'|\mathbf{X}}(\mathbf{x}' \mid \mathbf{x})\phi(\mathbf{x}) = \prod_{i=1}^{n} p_{X_i'|X_i}(x_i' \mid x_i)\phi(x_i) = \prod_{i=1}^{n} p_{X_i'|X_i}(x_i \mid x_i')\phi(x_i') = p_{\mathbf{X}'|\mathbf{X}}(\mathbf{x} \mid \mathbf{x}')\phi(\mathbf{x}') \tag{16}$$

3.2. Intrinsic parameter

The parameter κ (omitting index i for simplicity) in (11) determines the limiting algorithm and is an intrinsic characteristic of the proposal PDF. Figure 1 shows the variation of κ and the associated parameters a and s (omitting index i) with the standard deviation s_0 of the proposal PDF. The results for two commonly used proposal PDF, Gaussian and uniform, are shown. Note that a uniform proposal PDF on $[X-w, X+w]$ around the current sample X has a standard deviation of $s_0 = w/\sqrt{3}$. For both types of PDF there is a lower limit for a (near 0.6) and an upper limit for s (near 0.8). These limits arise from the distribution type and not from the inequalities in (12). Choosing directly the parameters a and s ($a^2 + s^2 = 1$) rather than the proposal PDF potentially offers more flexibility in tuning the algorithm.

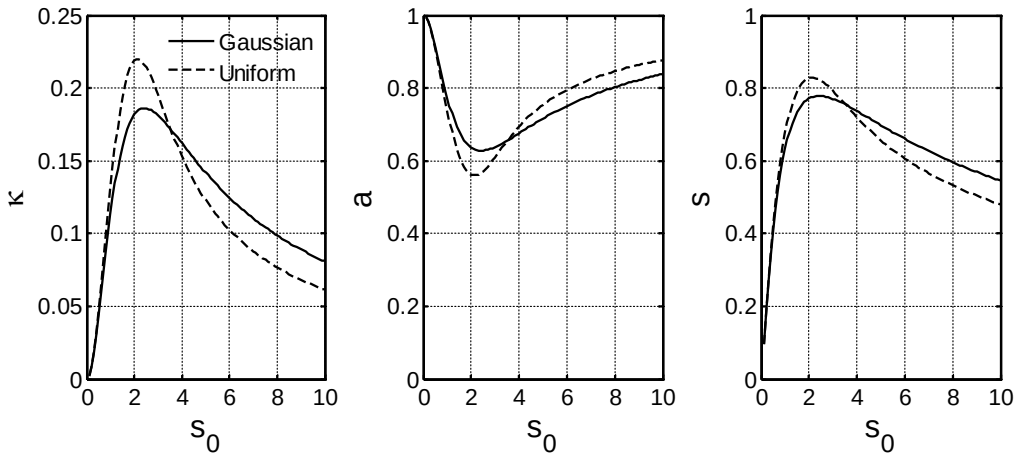

Figure 1. Variation of κ, a and s with standard deviation s_0 of proposal PDF

3.3. Generalized concept

The equality $a^2 + s^2 = 1$ that imposes constraint on the mean and variance of the candidate X' is highly non-trivial to reason from first principle based on the independent-component MCMC algorithm. Not only does the derivation in the last section show the transition PDF $p_{X'|X}(\cdot|\cdot)$ satisfies detailed balance, it also reveals a new perspective for generating correlated but identically distributed standard Gaussian samples without explicitly using MCMC. Specifically, starting with a standard Gaussian sample X, one may ask, is it possible to generate another standard Gaussian sample X' that is correlated to X by simply generating it as a Gaussian random variable whose mean and variance can possibly depend on X? The derivation shows that the

answer is positive. Remarkably, the mean is just a fraction a of X and the variance is a constant independent of X, and they must satisfy the constraint $a^2 + s^2 = 1$.

4. Illustrative examples

In this section we present three examples to illustrate numerically the behavior of the independent-component MCMC algorithm for the equivalent problem with hidden variables, i.e., Algorithm I in Section 2.1. In the first two examples the number of random variables in the original problem is small, one in the first and seven in the second. In the third example there is one variable with multiplicative effect on the response, in addition to a large number of variables each having an infinitesimal effect. We shall demonstrate numerically that as the number of hidden variables increases Algorithm I behaviors asymptotically as Algorithm II (the limiting algorithm). Note that in reality one should implement Algorithm II rather than Algorithm I with a large number of hidden variables. The latter is performed here only for illustration.

In the implementation of Subset Simulation, it is assumed that $p_0 = 0.1$ (level probability) and $N = 1000$ (number of samples per level). Three simulation levels (0,1,2) are performed, corresponding to target probabilities of 0.1, 0.01 and 0.001. The proposal PDF for all standard Gaussian variables and for all simulation levels is chosen as uniform distribution centered at the current sample with a maximum step length of $w = 1$. This corresponds to a standard deviation of $s_0 = w/\sqrt{3} \approx 0.58$ associated with the proposal PDF and a standard deviation of $s \approx 0.47$ (see Figure 1) of the candidate from the current sample.

4.1. Standard Gaussian response

Consider the failure probability defined as $P(Y > b)$ where $Y = X$ and X is standard Gaussian. Clearly the number of random variables in the original problem is $n = 1$. In the equivalent problem, X is represented by $X = \sum_{j=1}^{n'} Z_j / \sqrt{n'}$, where $\{Z_j\}_{j=1}^{n'}$ are i.i.d. standard Gaussian hidden variables and n' is their number.

Figure 2 shows selected statistics Algorithm I, estimated with 1000 independent runs. In Figure 2(a), the dashed line shows the acceptance probability in Step I. The solid line shows

the (conditional) acceptance probability in Step II given that the candidate is accepted in Step I. The product of these two probabilities gives the (unconditional) acceptance probability of the candidate as the next conditional failure sample. These probabilities are estimated from transitions between successive samples at each simulation level in each run and then averaged over the 1000 runs. The results for simulation levels 0, 1 and 2 are denoted by 'x', 'o' and diamond. For simulation level 0 ('x') the acceptance probability in Step I is trivially 1 because no MCMC is involved. For simulation levels 1 ('o') and 2 (diamond), the acceptance probability in Step I (dashed line) quickly rises to 1 as the number of hidden variables n' increases. This increase is geometric in nature because to reject the n'-dimensional candidate in Step I it is required to reject the candidates in all the n' components. The acceptance probability in Step II (solid line) is insensitive to n', although a slight increase is observed.

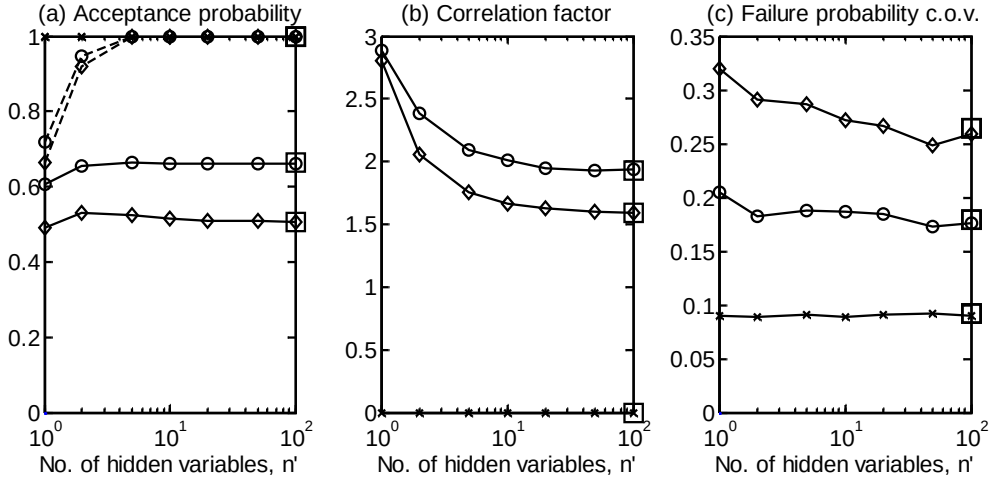

Figure 2. Variation of (a) acceptance probability, (b) correlation factor and (c) c.o.v. of failure probability estimate with number of hidden variables n' for Algorithm I. 'x', 'o', diamond – simulation level 0, 1, 2. Square – Algorithm II. In (a), dashed line – probability of candidate accepted in Step I; solid line – probability of candidate accepted in Step II given that it is accepted in Step I

Figure 2(b) shows the correlation factor γ_i at different simulation levels ($i = 0,1,2$). Recall that [12] $\gamma_i = 2\sum_{k=1}^{N_s-1}(1-k/N_s)\rho_i(k)$ where $N_s = 1/p_0$ is the number of samples per chain and $\rho_i(k)$ is the correlation coefficient of the indicator functions of failure at k steps apart. The correlation coefficients and hence the correlation factor are estimated using the samples in the simulation. The correlation factor is presented as it directly affects efficiency. For example, if the samples at different levels are uncorrelated, the coefficient of variation (c.o.v.=standard deviation/mean) of the failure probability estimate at level i is

approximately equal to $\alpha_i = [\sum_{j=0}^{i}(1+\gamma_j)(1-p_0)/p_0 N]^{1/2}$. In Figure 2(b), the correlation factor is trivially zero at simulation level 0 ('x', Direct Monte Carlo). At other levels it shows a moderate decrease with n', even though the acceptance probability in Step II (solid line, Figure 2(a)) is relatively constant. This suggests that increasing n' may reduce the spatial correlation between the current sample and the candidate when it is accepted.

Figure 2(c) shows the c.o.v. of the failure probability estimates at the three simulation levels. Recall that a Subset Simulation run produces estimates of threshold levels corresponding to fixed target failure probabilities, rather than estimates of failure probabilities at fixed threshold levels. To obtain the c.o.v. at fixed threshold levels, as shown in Figure 2(c), the 'reference' (close to exact) threshold levels corresponding to fixed probabilities are obtained by averaging those from the 100 simulation runs. They are then interpolated to yield the reference threshold levels at failure probabilities 0.1, 0.01 and 0.001. The failure probability estimates of each simulation run at these threshold levels are obtained by interpolating the results in the run. For each threshold level calculating the sample c.o.v. of the failure probability estimates among the 100 runs yields the values shown in Figure 2(c). It is seen that the c.o.v. generally decreases with n', although the extent is small.

The results obtained by Algorithm II are shown on the right end of Figure 2(a) to (c). They coincide visually with the results of Algorithm I for $n' = 100$. This is expected because Algorithm II is theoretically equivalent to Algorithm I for $n' \to \infty$. Comparing Algorithm II with Algorithm I with no additional hidden variables ($n' = 1$), for simulation level 3 (probability 0.001), the ratio of c.o.v. is 0.26/0.32 = 81%, i.e., a ratio of $(0.81)^2$=66% in the required number of samples to achieve the same accuracy.

4.2. Moment resisting frame

Consider a moment resisting frame with uncertainty in moment capacities $\theta_1,...,\theta_5$ at the joints and in the loads θ_6 and θ_7, as shown in Figure 3 [33]. These non-Gaussian random variables are represented by mapping standard Gaussian random variables $X_1,...,X_7$ to uniform variates on [0,1] and then to the target distribution via the inverse of their CDF. In the equivalent problem, X_i is further represented by n' hidden variables $\{Z_{ij}\}_{j=1}^{n'}$ as

$X_i = \sum_{j=1}^{n'} Z_{ij} / \sqrt{n'}$. The number of random variables is thus $7n'$. Failure is defined as collapse in any one of the three modes shown in Figure 3. This can be written as $\{Y > 1\}$ where $Y = \max\{g_1, g_2, g_3\}$ and g_i s are the (dimensionless) load to capacity ratios, which can be obtained by limit equilibrium as

$$g_1 = \frac{5\theta_6 + 5\theta_7}{\theta_1 + 2\theta_3 + 2\theta_4 + \theta_5} \qquad g_2 = \frac{5\theta_6}{\theta_1 + 2\theta_2 + \theta_4 + \theta_5} \qquad g_3 = \frac{5\theta_7}{\theta_2 + 2\theta_3 + \theta_4} \tag{17}$$

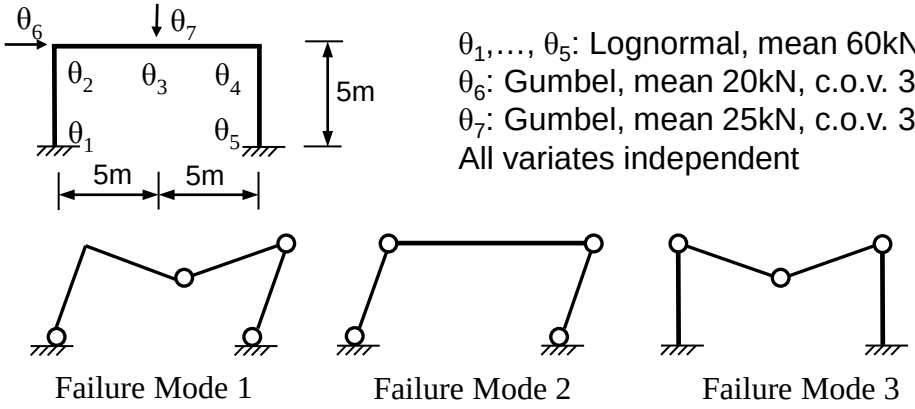

Figure 3 Moment resisting frame problem

Figure 4 shows the statistics of Algorithm I estimated using 1000 independent runs, analogous to Figure 2. In Figure 4(a) the acceptance probability in Step I is saturated at 1 when $n' = 1$ because in this case there are already seven variables in the problem. Different from Figure 2(a), there is a slight decrease (rather than increase) in the acceptance probability in Step II (solid lines) with n'. This reveals the problem-dependent effect of the number of hidden variables on the success rate of candidate lying in the failure region. Similar to Figure 2(b), the correlation factor in Figure 4(b) shows a decreasing trend with n', suggesting a positive effect on reducing the spatial correlation between the candidate and the current sample.

Similar to Figure 2(c), the c.o.v. of failure probability estimate in Figure 4(c) shows a small decrease with n'. The results for Algorithm II (square) coincide with those for $n' = 100$. Comparing Algorithm II with Algorithm I with no additional hidden variables ($n' = 1$), for simulation level 3 the ratio of c.o.v. is 0.27/0.325 = 83%, i.e., a ratio of $(0.83)^2$ = 69% in the required number of samples to achieve the same accuracy. This is similar to the last example.

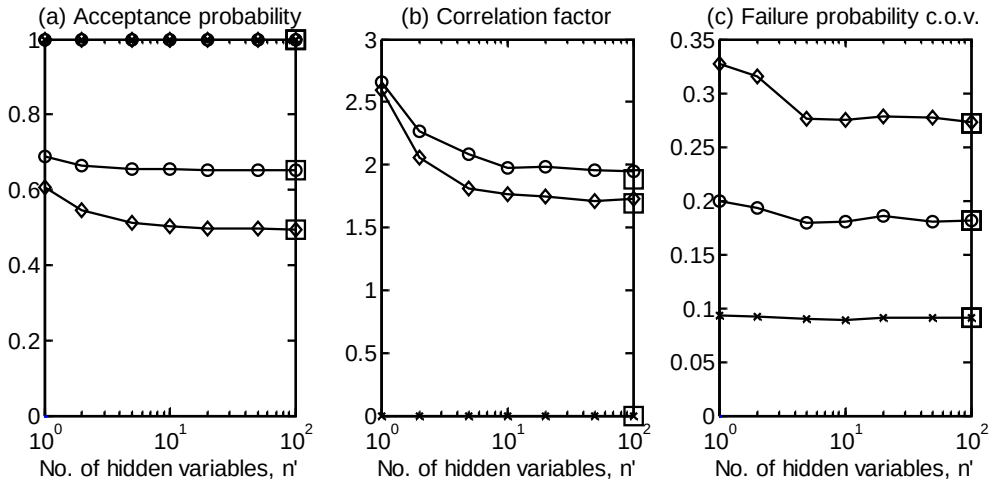

Figure 4. Variation of (a) acceptance probability, (b) correlation factor and (c) c.o.v. of failure probability estimate with number of hidden variables n' for Algorithm I. Same legend as Figure 2

4.3. First passage problem with uncertain excitation intensity

Consider a single-degree-of-freedom structure starting from rest and subjected to white noise excitation. The displacement $y(t)$ satisfies the following governing equation:

$$\ddot{y}(t) + 2\zeta\omega\dot{y}(t) + \omega^2 y(t) = W(t) \tag{18}$$

where $\omega = 2\pi$ rad/sec is the natural frequency, $\zeta = 2\%$ is the damping ratio and $W(t)$ is white noise with power spectral density (PSD, one-sided) S (N^2/Hz). The PSD S is exponentially distributed with mean $S_0 = 0.001\mathrm{N}^2/\mathrm{Hz}$. The excitation is generated in discrete time by $W(j\Delta t) = \sqrt{S/2\Delta t}\,Z_{1j}$ ($j = 1,2,\ldots$), where $\Delta t = 0.05$ sec is the time interval and $\{Z_{1j}\}_{j=1,2,\ldots}$ are i.i.d. standard Gaussian. Failure is defined as the exceedance of $|y(t)|$ over threshold b at any time instant between 0 to 10 sec, i.e., $F = \{\max_{j=1,\ldots,n_t} |y(t_j)| > b\}$ where $n_t = 10/0.05 = 200$.

The random variables in the original problem comprise the exponentially distributed PSD S and i.i.d. standard Gaussian $\{Z_{1j}\}_{j=1}^{n_t}$ that represent the excitation. Note that S is only a single variable but it has a multiplicative effect on the response. On the other hand, $\{Z_{1j}\}_{j=1}^{n_t}$ appear in large number but each has an additive and infinitesimal effect on the response. In the equivalent problem we represent S by i.i.d. standard Gaussian

hidden variables $\{Z_{2j}\}_{j=1}^{n'}$ as $S = -S_0 \ln \Phi(\sum_{j=1}^{n'} Z_{2j} / \sqrt{n'})$, which can be verified using inversion principle to give an exponentially distributed variate with mean S_0. The random variables in the equivalent problem therefore comprise $\{Z_{1j}\}_{j=1}^{n_t}$ and $\{Z_{2j}\}_{j=1}^{n'}$, and their total number is $n_t + n'$ ($n_t = 200$).

Figure 5 shows the statistics of Algorithm I estimated using 1000 independent runs, analogous to Figure 2. In Figure 5(a) the acceptance probability in Step I is saturated at 1 when $n' = 1$ because in this case there are already 201 variables in the problem. The acceptance probability in Step II (solid line) is insensitive to n'. The same is also true for the correlation factor in Figure 5(b) and the c.o.v. of failure probability estimate in Figure 5(c). To within statistical error the results for Algorithm II (square) are similar to those for $n' = 100$. The efficiency of Algorithm II is practically the same as Algorithm I with no additional hidden variables ($n' = 1$).

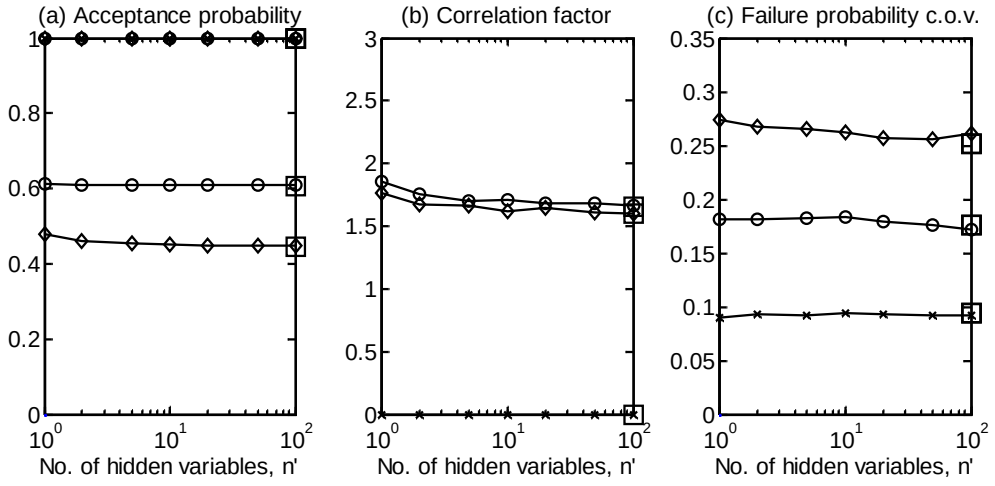

Figure 5. Variation of (a) acceptance probability, (b) correlation factor and (c) c.o.v. of failure probability estimate with number of hidden variables n' for Algorithm I. Same legend as Figure 2

5. Derivation of limiting behavior

In this section we derive the limiting expression ($n' \to \infty$) for the conditional PDF $p_{X_i'|X_i}(x_i' \mid x_i)$ in (8) according to the algorithm in Section 2.1. Clearly, this PDF depends on the proposal PDF p_i^* but the functional form will be identical for different i.

It does not depend on the failure event because X_i is given. It is therefore sufficient to study $p_{X_i'|X_i}(x_i'|x_i)$ for a generic i. To simplify notation, we shall omit the index i in the derivation. That is, the PDF shall be denoted by $p_{X'|X}(x'|x)$, the proposal PDF shall be denoted by p^*; and X_i shall be denoted by

$$X = \frac{1}{\sqrt{n'}} \sum_{j=1}^{n'} Z_j \tag{19}$$

where $\{Z_j\}_{j=1}^{n'}$ are hidden variables. Similarly, X_i' shall be denoted by

$$X' = \frac{1}{\sqrt{n'}} \sum_{j=1}^{n'} Z_j' \tag{20}$$

Here, $\{Z_j'\}_{j=1}^{n'}$ are the candidates of hidden variables generated according to the following, adapted from the inner loop of the algorithm in Section 2.1 (omitting index i):

For $j = 1,...,n'$

1. Generate ξ_j from the proposal PDF $p^*(\xi_j - Z_j)$ and U_j uniformly on [0,1].
2. Calculate $r_j = \phi(\xi_j)/\phi(Z_j)$.

   Set $Z_j' = \xi_j$ if $U_j \le r_j$. Otherwise set $Z_j' = Z_j$.

End j

We shall first study the PDF of $\{Z_j\}_{j=1}^{n'}$ conditional on $X = x$. We then obtain the conditional PDF of X' by analyzing the transition from Z_j to Z_j' ($j = 1,...,n'$). The latter is analytically intractable for each j but their overall effect on X' is manageable in the limit as $n' \to \infty$.

5.1. Conditional distribution of hidden variables

Unconditionally, $\{Z_j\}_{j=1}^{n'}$ are i.i.d. standard Gaussian. The condition $X = x$ imposes a linear constraint $\sum_{j=1}^{n'} Z_j / \sqrt{n'} = x$ on the standard Gaussian vector $\mathbf{Z} = [Z_1,...,Z_n]^T$. This constraint can be written as

474 $\mathbf{b}^T\mathbf{Z} = x \qquad \mathbf{b} = \frac{1}{\sqrt{n'}}[1,...,1]^T = \frac{1}{\sqrt{n'}}\mathbf{1}$ (21)

475 where $\mathbf{1} = [1,...,1]^T$ is an n'-by-1 vector of ones. Let $\{\mathbf{a}_j \in R^{n'}\}_{j=1}^{n'}$ be an orthonormal
476 basis with $\mathbf{a}_1 = \mathbf{b}$. By rotational symmetry of standard Gaussian vectors, if there is no
477 constraint we can write $\mathbf{Z} = \sum_{k=1}^{n'} \xi_k \mathbf{a}_k$ where $\boldsymbol{\xi} = [\xi_1,..., \xi_{n'}]^T$ is an i.i.d. standard
478 Gaussian vector. Note that $\mathbf{b}^T\mathbf{Z} = \sum_{k=1}^{n'} \xi_k \mathbf{a}_1{}^T\mathbf{a}_k = \xi_1$ since $\mathbf{a}_1^T\mathbf{a}_1 = 1$ and $\mathbf{a}_1^T\mathbf{a}_k = 0$ for
479 $k = 2,..., n'$. This means that (21) only imposes a constraint on ξ_1, being $\xi_1 = x$, while
480 $\{\xi_2,..., \xi_{n'}\}$ remain unconstrained. The vector $\mathbf{Z}$ under (21) can therefore be represented
481 as the sum of $x\mathbf{b}$ and a standard Gaussian vector in the orthogonal complement of $\mathbf{b}$.
482 The latter can be obtained by taking out the projection along $\mathbf{b}$ from $\boldsymbol{\xi}$, i.e., $\boldsymbol{\xi} - (\mathbf{b}^T\boldsymbol{\xi})\mathbf{b}$.
483 As a result,

484 $$\mathbf{Z} = x\mathbf{b} + [\boldsymbol{\xi} - (\mathbf{b}^T\boldsymbol{\xi})\mathbf{b}] = (\frac{x}{\sqrt{n'}} - \frac{1}{n'}\sum_{k=1}^{n'} \xi_k)\mathbf{1} + \boldsymbol{\xi} \quad (22)$$

485 after substituting $\mathbf{b} = \mathbf{1}/\sqrt{n'}$. Reading the j-th component of $\mathbf{Z}$,

486 $$Z_j = \frac{x}{\sqrt{n'}} + \xi_j - \frac{1}{n'}\sum_{k=1}^{n'} \xi_k \quad (23)$$

487 Using this representation, it can be established that $\{Z_j\}_{j=1}^{n'}$ are jointly Gaussian with
488 $E[Z_j \mid X = x] = x/\sqrt{n'}$, $\text{var}[Z_j \mid X = x] = 1 - 1/n'$ and conditional covariance
489 $\text{cov}[Z_j, Z_k \mid X = x] = -1/n'$ ($j \neq k$). Consequently,

490 $$p_{\mathbf{Z}|X=x}(\mathbf{z}) = (2\pi)^{-n'/2} |\mathbf{C}|^{-1/2} \exp[-\frac{1}{2}(\mathbf{z} - \frac{x}{\sqrt{n'}}\mathbf{1})^T \mathbf{C}^{-1}(\mathbf{z} - \frac{x}{\sqrt{n'}}\mathbf{1})] \quad (24)$$

491 where $\mathbf{C} = \mathbf{I} - n'^{-1}\mathbf{1}\mathbf{1}^T$ is the covariance matrix and $\mathbf{I} \in R^n$ denotes the identity matrix.
492 Correspondingly,

493 $$p_{Z_j|X=x}(z_j) = \frac{1}{\sqrt{2\pi(1-1/n')}} \exp[-\frac{1}{2}(z_j - \frac{x}{\sqrt{n'}})^2] \quad (25)$$

494 $$p_{Z_j Z_k|X=x}(z_j, z_k) = (2\pi)^{-1}(1-\frac{2}{n'})^{-1/2} \exp[-\frac{1}{2}(z_j - \frac{x}{\sqrt{n'}})^2 - \frac{1}{2}(z_k - \frac{x}{\sqrt{n'}})^2 - \frac{1}{2n'}(z_j + z_k - \frac{2x}{\sqrt{n'}})^2] \quad (26)$$

Using a Taylor series with respect to the small parameter $\varepsilon = 1/\sqrt{n'}$, it can be shown that, as $n' \to \infty$,

$$p_{Z_j|X=x}(z) \sim \phi(z)\{1 + \frac{x}{\sqrt{n'}} z + \frac{1}{2n'}[x^2(z^2-1)+2]\} \tag{27}$$

$$p_{Z_j Z_k|X=x}(z_j, z_k) \sim \phi(z_j)\phi(z_k)\{1 + \frac{x}{\sqrt{n'}}(z_j + z_k) + \frac{x^2-1}{2n'}[(z_j+z_k)^2 - 2]\} \tag{28}$$

where '~' reads 'asymptotic to', denoting mathematically that the ratio of the LHS to the RHS is equal to 1 in the limit. These asymptotic expressions shall be used for deriving the limiting behavior of X' in the next subsection.

5.2. Conditional distribution of X'

According to the algorithm,

$$X' = \frac{1}{\sqrt{n'}} \sum_{j=1}^{n'} Z'_j \tag{29}$$

where Z'_j is the candidate for Z_j. It can be represented as

$$Z'_j = Z_j + I_j W_j \tag{30}$$

where W_j is the random increment from Z_j and is distributed as the proposal PDF p^*; $I_j = I(U_j < \phi(Z_j + W_j)/\phi(Z_j))$ is the indicator function of acceptance; and U_j is uniformly distributed on $[0,1]$. The indicator function depends on Z_j, W_j and U_j, which are mutually independent. Given $X = x$, the conditional PDF of Z_j is given by (25). Correspondingly,

$$X' = x + \frac{1}{\sqrt{n'}} \sum_{j=1}^{n'} I_j W_j \qquad (X = x) \tag{31}$$

5.2.1. Expectation

Taking conditional expectation on (31),

$$E[X' | X = x] = x + \frac{1}{\sqrt{n'}} \sum_{j=1}^{n'} E[I_j W_j \mid X = x] \tag{32}$$

Asymptotic expressions ($n' \to \infty$) for expectations involving the products of I_j and W_j are analyzed in Section 8. It is shown in Section 8.1 that $E[I_j W_j \mid X = x] \sim -2\kappa x / \sqrt{n'}$ where $\kappa = \int_0^\infty w^2 p^*(w)\Phi(-w/2)dw$ as in (11). Substituting into (32),

$$E[X' \mid X = x] \sim (1 - 2\kappa)x = ax \tag{33}$$

where $a = 1 - 2\kappa$ as in (9). It is shown in Section 10 that $0 \le \kappa \le 1$, which implies $-1 \le a \le 1$.

5.2.2. Variance

Taking conditional variance on (31),

$$\mathrm{var}[X' \mid X = x] = \frac{1}{n'} \sum_{j=1}^{n'} \sum_{k=1}^{n'} \mathrm{cov}[I_j W_j, I_k W_k \mid X = x] \tag{34}$$

where $\mathrm{cov}[I_j W_j, I_k W_k \mid X = x]$ denotes the conditional covariance between $I_j W_j$ and $I_k W_k$. Note that

$$\begin{aligned} &\mathrm{cov}[I_j W_j, I_k W_k \mid X = x] \\ &= E[I_j W_j I_k W_k \mid X = x] - E[I_j W_j \mid X = x] E[I_k W_k \mid X = x] \qquad (35) \\ &\sim E[I_j W_j I_k W_k \mid X = x] - 4\kappa^2 \frac{x^2}{n'} \end{aligned}$$

since $E[I_j W_j \mid X = x] \sim -2\kappa x / \sqrt{n'}$. Substituting (35) into (34) gives

$$\mathrm{var}[X' \mid X = x] \sim \frac{1}{n'} \sum_{j=1}^{n'} \sum_{k=1}^{n'} E[I_j W_j I_k W_k \mid X = x] - 4\kappa^2 x^2 \tag{36}$$

The double sum can be evaluated by separating the terms for $j = k$ and $j \ne k$:

$$\frac{1}{n'} \sum_{j=1}^{n'} \sum_{k=1}^{n'} E[I_j W_j I_k W_k \mid X = x] = \frac{1}{n'} \sum_{j=1}^{n'} E[I_j W_j^2 \mid X = x] + \frac{1}{n'} \sum_{j \ne k}^{n'} E[I_j W_j I_k W_k \mid X = x] \tag{37}$$

Since $\{I_j W_j : j = 1,\ldots,n'\}$ are identically distributed and have the same correlation among each other,

$$E[I_j W_j^2 \mid X = x] = E[I_1 W_1^2 \mid X = x] \qquad j = 1,\ldots,n' \tag{38}$$

$$E[I_j W_j I_k W_k \mid X = x] = E[I_1 W_1 I_2 W_2 \mid X = x] \qquad j \ne k \tag{39}$$

Substituting into (37),

$$\frac{1}{n'}\sum_{j=1}^{n'}\sum_{k=1}^{n'} E[I_j W_j I_k W_k \mid X = x]$$

$$= \frac{1}{n'} n' E[I_1 W_1^2 \mid X = x] + \frac{1}{n'}(n'^2 - n') E[I_1 W_1 I_2 W_2 \mid X = x] \quad (40)$$

$$\sim E[I_1 W_1^2 \mid X = x] + n' E[I_1 W_1 I_2 W_2 \mid X = x]$$

It is shown in Sections 8.2 and 8.3 that $E[I_1 W_1^2 \mid X = x] \sim 4\kappa$ and $E[I_1 W_1 I_2 W_2 \mid X = x] \sim 4\kappa^2 (x^2 - 1)/n'$. Substituting into (40) and then the resulting expression into (36) gives

$$\mathrm{var}[X' \mid X = x] \sim 4\kappa - 4\kappa^2 \quad (41)$$

Surprisingly, the variance of X' does not depend on X. Since $0 \le \kappa \le 1$, the expression on the RHS of (41) is always positive.

5.2.3. Central Limit Theorem

Recall from (31) that, given $X = x$, we can write $X' = x + \sum_{j=1}^{n'} I_j W_j / n'$. Note that $\{I_j W_j\}_{j=1}^{n'}$ is a sequence of identically distributed but correlated random variables. As $n' \to \infty$, X' is asymptotically Gaussian if the proposal PDF has finite variance, i.e., $E[W_j^2] < \infty$. This can be shown using the Central Limit Theorem for correlated random variables [34], which requires $E[|I_j W_j| \mid X = x] < \infty$ and $\mathrm{var}[I_j W_j \mid X = x] < \infty$ ($j = 1, ..., n'$) for every n'; and $\mathrm{var}[X' \mid X = x] < \infty$ as $n' \to \infty$. The first two conditions can be established using Cauchy-Schwartz inequality:

$$E[|I_j W_j| \mid X = x] \le E[I_j^2 \mid X = x]^{1/2} E[W_j^2 \mid X = x]^{1/2} \le E[W_j^2]^{1/2} < \infty \quad (42)$$

$$\mathrm{var}[I_j W_j \mid X = x] \le E[I_j^2 W_j^2 \mid X = x] \le E[W_j^2 \mid X = x] = E[W_j^2] < \infty \quad (43)$$

where we have used the fact that $0 \le I_j \le 1$ and W_j does not depend on X. The last condition on the asymptotic variance of X' follows directly from (41) that $\mathrm{var}[X' \mid X = x] = 4\kappa - 4\kappa^2 < \infty$ as $n' \to \infty$.

562 *5.2.4. Detailed balance*

563 Since each Z'_j is generated according to MCMC, the one-dimensional PDF $p_{Z'_j|Z_j}(\cdot|\cdot)$

564 satisfies detailed balance with a stationary PDF $\phi(\cdot)$:

565 $$p_{Z'_j|Z_j}(z'_j \mid z_j)\phi(z_j) = p_{Z'_j|Z_j}(z_j \mid z'_j)\phi(z'_j) \tag{44}$$

566 As a result the joint conditional PDF $p_{\mathbf{Z}'|\mathbf{Z}}(\mathbf{z}' \mid \mathbf{z})$ also satisfies detailed balance with a

567 stationary joint PDF $\phi(\cdot)$:

568 $$p_{\mathbf{Z}'|\mathbf{Z}}(\mathbf{z}' \mid \mathbf{z})\phi(\mathbf{z}) = p_{\mathbf{Z}'|\mathbf{Z}}(\mathbf{z} \mid \mathbf{z}')\phi(\mathbf{z}') \tag{45}$$

569 The above argument stems directly from the original independent-component algorithm.

570

571 The transition PDF from X to X' also satisfies detailed balance with the stationary

572 PDF $\phi(\cdot)$:

573 $$p_{X'|X}(x' \mid x)\phi(x) = p_{X'|X}(x \mid x')\phi(x') \tag{46}$$

574 This can be shown as follow. From the foregoing results, given $X = x$, X' is

575 asymptotically Gaussian with mean $ax = (1-2\kappa)x$ and variance $s^2 = 4\kappa - 4\kappa^2$. That is,

576 $$p_{X'|X}(x' \mid x) = \frac{1}{\sqrt{2\pi}s}\exp[-\frac{1}{2s^2}(x'-ax)^2] \qquad n' \to \infty \tag{47}$$

577 Starting from the LHS of (46) and using (47),

578 $$\begin{aligned} p_{X'|X}(x' \mid x)\phi(x) &= \frac{1}{\sqrt{2\pi}s}\exp[-\frac{1}{2s^2}(x'-ax)^2]\times\frac{1}{\sqrt{2\pi}}\exp(-\frac{1}{2}x^2) \\ &= \frac{1}{2\pi s}\exp\{-\frac{1}{2}[\frac{(x'-ax)^2}{s^2}+x^2]\} \end{aligned} \tag{48}$$

579 Completing the square on x, the term in the exponent can be written as

580 $$\frac{(x'-ax)^2}{s^2}+x^2 = \frac{a^2+s^2}{s^2}(x-\frac{ax'}{a^2+s^2})^2+\frac{x'^2}{a^2+s^2} \tag{49}$$

581 Substituting into (48) gives

582 $$p_{X'|X}(x' \mid x)\phi(x) = \frac{1}{\sqrt{2\pi}s}\exp[-\frac{a^2+s^2}{2s^2}(x-\frac{ax'}{a^2+s^2})^2]\times\frac{1}{\sqrt{2\pi}}\exp(-\frac{1}{2}\frac{x'^2}{a^2+s^2}) \tag{50}$$

583 This is equal to $p_{X'|X}(x \mid x')\phi(x')$, i.e., the RHS of (46), if and only if $a^2+s^2=1$. This

584 condition is always satisfied because $a^2+s^2 = (1-2\kappa)^2+4\kappa-4\kappa^2 = 1$.

585

6. Conclusions

By setting up an equivalent problem with arbitrary number of hidden variables for any given problem, we have investigated the limiting behavior of the independent-component MCMC algorithm (Algorithm I) for generating failure samples, which is conventionally used in Subset Simulation for risk assessment of rare events in complex systems. The results are remarkably simple and they lead to a simple limiting algorithm (Algorithm II) for generating failure samples. The choice of the proposal distribution is no longer relevant and the algorithm is directly controlled through the standard deviation of the candidate from the current sample. The limiting algorithm coincides with a method [31] recently proposed by independent researchers, where a joint Gaussian distribution was ingeniously imposed. The present paper provides theoretical reasoning and insights into the method.

The numerical examples demonstrate the effect of the number of hidden variables in the equivalent problem and the convergence of results to the limiting algorithm. For the examples presented there is only a small reduction in the c.o.v. of the failure probability estimate brought by the limiting algorithm. The significance of the algorithm lies in its simplicity and the general discovery that the candidate can in fact be generated as a Gaussian vector whose statistics depend on the current sample. This offers new perspectives and possibilities for increasing efficiency by tuning the statistics a priori or adaptively based on accumulated samples. Development along this line can be found in [31].

7. Acknowledgements

The work described in this paper is partially supported by University of Liverpool Grant EGG10034 and a grant from the Research Grants Council of the Hong Kong Special Administrative Region, China (Project No. CityU8/CRF/13G).

References

[1] Zio E. Reliability engineering: Old problems and new challenges. Reliability Engineering & System Safety 2009;94:125–41.

[2] Berger J, Buckle I, Greene M. The 2010 Canterbury and 2011 Christchurch New Zealand Earthquakes and the 2011 Tohoku Japan Earthquake : Emerging Research Needs and Opportunities, Earthquake Engineering Research Institute, CA, 2012.
[3] Aven T, Krohn BS. A new perspective on how to understand, assess and manage risk and the unforeseen. Reliability Engineering and System Safety 2014;121:1–10.
[4] Devroye L. Non-uniform random variate generation, Springer Verlag, New York. 1985.
[5] Rubinstein RY. Systems, Models, Simulation, and the Monte Carlo Methods. Simulation and the Monte Carlo Method, NY, 1981.
[6] Jun S. Liu. Monte Carlo Strategies in Scientific Computing, Springer, NY, 2001.
[7] Robert CP, Casella G. Monte Carlo Statistical Methods, Springer, NY, 2004.
[8] Schuëller GI, Pradlwarter HJ, Koutsourelakis PS. A critical appraisal of reliability estimation procedures for high dimensions. Probabilistic Engineering Mechanics 2004;19:463–74.
[9] Schuëller GI, Pradlwarter HJ. Benchmark study on reliability estimation in higher dimensions of structural systems – An overview. Structural Safety 2007;29:167–82.
[10] Au SK, Beck JL. Important sampling in high dimensions. Structural Safety 2003;25:139–63.
[11] Katafygiotis LS, Zuev KM. Geometric insight into the challenges of solving high-dimensional reliability problems. Probabilistic Engineering Mechanics 2008;23:208–18.
[12] Au SK, Beck JL. Estimation of small failure probabilities in high dimensions by subset simulation. Probabilistic Engineering Mechanics 2001;16:263–77.
[13] Au SK, Beck JL. Subset Simulation and its Application to Seismic Risk Based on Dynamic Analysis. Journal of Engineering Mechanics 2003;129:901–17.
[14] Au SK, Cao ZJ, Wang Y. Implementing advanced Monte Carlo simulation under spreadsheet environment. Structural Safety 2010;32:281–92.
[15] Au SK, Wang Y. Engineering Risk Assessment with Subset Simulation, John Wiley & Sons, Singapore, 2014.
[16] Au SK. Reliability-based design sensitivity by efficient simulation. Computers and Structures, vol. 83, 2005, p. 1048–61.
[17] Ching J, Hsieh Y-H. Local estimation of failure probability function and its confidence interval with maximum entropy principle. Probabilistic Engineering Mechanics 2007;22:39–49.
[18] Song S, Lu Z, Qiao H. Subset simulation for structural reliability sensitivity analysis. Reliability Engineering & System Safety 2009;94:658–65.

[19] Jensen HA. Structural optimization of linear dynamical systems under stochastic excitation: a moving reliability database approach. Computer Methods in Applied Mechanics and Engineering 2005;194:1757–78.

[20] Ching J, Hsieh Y-H. Approximate reliability-based optimization using a three-step approach based on subset simulation. Journal of Engineering Mechanics 2007;133:481–93.

[21] Li H-S, Au S-K. Design optimization using Subset Simulation algorithm. Structural Safety 2010;32:384–92.

[22] Taflanidis AA, Beck JL. Stochastic subset optimization for reliability optimization and sensitivity analysis in system design. Computers & Structures 2009;87:318–31.

[23] Dubourg V, Sudret B, Bourinet J-M. Reliability-based design optimization using kriging surrogates and subset simulation. Structural and Multidisciplinary Optimization 2011;44:673–90.

[24] Wang Q, Lu Z, Zhou C. New topology optimization method for wing leading-edge ribs. Journal of Aircraft 2011;48:1741–8.

[25] Ching J, Beck JL, Au SK. Hybrid subset simulation method for reliability estimation of dynamical systems subject to stochastic excitation. Probabilistic Engineering Mechanics 2005;20:199–214.

[26] Katafygiotis L, Cheung SH. A two-stage subset simulation-based approach for calculating the reliability of inelastic structural systems subjected to Gaussian random excitations. Computer Methods in Applied Mechanics and Engineering 2005;194:1581–95.

[27] Au SK. Augmenting approximate solutions for consistent reliability analysis. Probabilistic Engineering Mechanics 2007;22:77–87.

[28] Zuev KM, Katafygiotis LS. Modified Metropolis–Hastings algorithm with delayed rejection. Probabilistic Engineering Mechanics 2011;26:405–12.

[29] Echard B, Gayton N, Lemaire M. AK-MCS: an active learning reliability method combining Kriging and Monte Carlo simulation. Structural Safety 2011;33:145–54.

[30] Papadopoulos V, Giovanis DG, Lagaros ND, Papadrakakis M. Accelerated subset simulation with neural networks for reliability analysis. Computer Methods in Applied Mechanics and Engineering 2012;223:70–80.

[31] Metropolis N, Rosenbluth AW, Rosenbluth MN et al. Equations of state calculations by fast computing machines. Journal of Chemical Physics 1953; 21:1087–91.

[32] Papaioannou I, Betz W, Zwirglmaier K, Straub D, MCMC algorithms for Subset Simulation, Probabilistic Engineering Mechanics 2015; 44:89-103.

[33] Schueller GI, Bucher CG, Bourgund, U, Quypornprasert W, On efficient computational schemes to calculate structural failure probabilities. Probabilistic Engineering Mechanics 1989; 4(1):10–18.

[34] DasGupta A. Asymptotic theory of statistics and probability. Springer, NY, 2008.

[35] Brookes M, The Matrix Reference Manual, /http://www.ee.ic.ac.uk/hp/staff/dmb/matrix/intro.htmlS, 2005 [online].

8. Appendix. Expectations involving I_j

In this appendix we derive the asymptotic expressions for $E[I_1 W_1 \mid X = x]$, $E[I_1 W_1^2 \mid X = x]$ and $E[I_1 W_1 I_2 W_2 \mid X = x]$. These expressions are used in Section 4. Since $\{I_j W_j\}_{j=1}^{n'}$ are i.i.d., the results can be used for $E[I_j W_j \mid X = x]$, $E[I_j W_j^2 \mid X = x]$ and $E[I_j W_j I_k W_k \mid X = x]$ ($j \neq k$).

8.1. Expression for $E[I_1 W_1 \mid X = x]$

Recall that $I_1 = I(U_1 < \phi(Z_1 + W_1)/\phi(Z_1))$, where U_1, W_1, Z_1 are mutually independent; U_1 is uniform on [0,1]; and W_1 is distributed as p^*. The condition $\{X = x\}$ does not affect the distribution of U_1 or W_1 but Z_1. From (27):

$$p_{Z_1|X=x}(z) \sim \phi(z)(1 + \frac{x}{\sqrt{n'}} z) \qquad n' \to \infty \qquad (51)$$

Using this expression,

$$\begin{aligned} & E[I_1 W_1 \mid X = x] \\ & = \iiint I(u < \frac{\phi(z+w)}{\phi(z)}) w \; p_{Z_1|X=x}(z) p^*(w) du dz dw \qquad (52) \\ & \sim \iiint I(u < \frac{\phi(z+w)}{\phi(z)}) w \phi(z) p^*(w) du dz dw + \frac{x}{\sqrt{n'}} \iiint I(u < \frac{\phi(z+w)}{\phi(z)}) w z \phi(z) p^*(w) du dz dw \end{aligned}$$

Let

$$J = I(U < \frac{\phi(V+W)}{\phi(V)}) \qquad (53)$$

be an indicator function variable where U, W and V are mutually independent; U is uniform on [0,1]; W is distributed as p^*; and V is a standard Gaussian. Then (52) can be written as

$$E[I_1 W_1 \mid X = x] \sim E[JW] + \frac{x}{\sqrt{n'}} E[JWV] \tag{54}$$

The expectations on the RHS no longer depend on x or n' and their determination is purely an integration problem. They are investigated in Section 9. It is shown that $E[JW] = 0$ and $E[JWV] = -2\kappa$ where $\kappa = \int_0^\infty w^2 p^*(w)\Phi(-w/2)dw$ as in (11). Substituting into (54) gives

$$E[I_1 W_1 \mid X = x] \sim -\frac{2\kappa x}{\sqrt{n'}} \qquad n' \to \infty \tag{55}$$

8.2. Expression for $E[I_1 W_1^2 \mid X = x]$

Using the same technique in Section 8.1,

$$E[I_1 W_1^2 \mid X = x] \sim E[JW^2] + \frac{x}{\sqrt{n'}} E[JW^2 V] \tag{56}$$

where U, V and W are defined as before. It is shown in Section 9 that $E[JW^2] = 4\kappa \neq 0$ and so it is the leading order term, giving

$$E[I_1 W_1^2 \mid X = x] \sim 4\kappa \qquad n' \to \infty \tag{57}$$

8.3. Expression for $E[I_1 W_1 I_2 W_2 \mid X = x]$

The expectation of $E[I_1 W_1 I_2 W_2 \mid X = x]$ involves the joint PDF of Z_1 and Z_2. Using (28),

$$p_{Z_1 Z_2 \mid X = x}(z_1, z_2) \sim \phi(z_1)\phi(z_2)\{1 + \frac{x}{\sqrt{n'}}(z_1 + z_2) + \frac{x^2 - 1}{2n'}[(z_1 + z_2)^2 - 2]\} \qquad n' \to \infty \tag{58}$$

Using this expression,

$$E[I_1 W_1 I_2 W_2 \mid X = x] \sim E[J_1 W_1 J_2 W_2] + \frac{x}{\sqrt{n'}} E[J_1 W_1 J_2 W_2 (V_1 + V_2)] + \frac{x^2 - 1}{2n'} E\{J_1 W_1 J_2 W_2 [(V_1 + V_2)^2 - 2]\} \tag{59}$$

where

732 $$J_k = I(U_k < \frac{\phi(V_k + W_k)}{\phi(V_k)}) \qquad k = 1,2 \qquad (60)$$

733 $U_1, U_2, V_1, V_2, W_1, W_2$ are mutually independent; U_1, U_2 are uniformly distributed on [0,1];

734 V_1, V_2 are standard Gaussian; W_1, W_2 are distributed as the proposal PDF p^*.

735

736 For the first term in (59),

737 $$E[J_1 W_1 J_2 W_2] = E[J_1 W_1] E[J_2 W_2] = 0 \qquad (61)$$

738 since $E[J_1 W_1] = E[J_2 W_2] = 0$ from Section 9. The second term is also zero because

739 $$E[J_1 W_1 J_2 W_2 V_1] = E[J_1 W_1 V_1] E[J_2 W_2] = E[J_1 W_1 V_1] \times 0 = 0 \qquad (62)$$

740 $$E[J_1 W_1 J_2 W_2 V_2] = E[J_1 W_1] E[J_2 W_2 V_2] = 0 \times E[J_2 W_2 V_2] = 0 \qquad (63)$$

741 For the third term in (59), note that

742 $$\begin{aligned} &E\{J_1 W_1 J_2 W_2 [(V_1 + V_2)^2 - 2]\} \\ &= E[J_1 W_1 J_2 W_2 V_1^2] + E[J_1 W_1 J_2 W_2 V_2^2] + 2E[J_1 W_1 J_2 W_2 V_1 V_2] - 2E[J_1 W_1 J_2 W_2] \end{aligned} \qquad (64)$$

743 The following shows that only the third term in (64) is non-zero:

744 $$E[J_1 W_1 J_2 W_2 V_1^2] = E[J_1 W_1 V_1^2] E[J_2 W_2] = E[J_1 W_1 V_1^2] \times 0 = 0 \qquad (65)$$

745 $$E[J_1 W_1 J_2 W_2 V_2^2] = E[J_1 W_1] E[J_2 W_2 V_2^2] = 0 \times E[J_2 W_2 V_2^2] = 0 \qquad (66)$$

746 $$E[J_1 W_1 J_2 W_2 V_1 V_2] = E[J_1 W_1 V_1] E[J_2 W_2 V_2] = E[J_1 W_1 V_1]^2 = 4\kappa^2 \qquad (67)$$

747 after using $E[J_1 W_1 V_1] = -2\kappa$ derived in Section 9. For the last term in (64),

748 $E[J_1 W_1 J_2 W_2] = 0$ as shown earlier in (61). Thus, $E\{J_1 W_1 J_2 W_2 [(V_1 + V_2)^2 - 2]\} = 4\kappa^2$.

749 Substituting into (59) gives

750 $$E[I_1 W_1 I_2 W_2 \mid X = x] \sim 4\kappa^2 \frac{x^2 - 1}{n} \qquad n' \to \infty \qquad (68)$$

751

752 **9. Appendix. Expectations involving J**

753 In this appendix we derive the expressions for $E[JW]$, $E[JWV]$ and $E[JW^2]$ where

754 $$J = I(U < \frac{\phi(V + W)}{\phi(V)}) \qquad (69)$$

is an indicator function variable; U, W and V are mutually independent; U is uniform on $[0,1]$, W is distributed as p^* and V is a standard Gaussian. The technique is outlined as follow. First, we integrate out U to obtain, for any p,q,

$$\begin{aligned} E[JW^pV^q] &= \iiint_0^1 I(u < \frac{\phi(v+w)}{\phi(v)}) w^p v^q \phi(v) p^*(w) du dv dw \\ &= \iint \min\{1, \frac{\phi(v+w)}{\phi(v)}\} w^p v^q \phi(v) p^*(w) dv dw \end{aligned} \tag{70}$$

To evaluate the double integral the domain of (v,w) is separated into D_1 and D_2:

$$D_1 = \{(v,w) \in R^2 : \frac{\phi(v+w)}{\phi(v)} > 1\} \qquad D_2 = \{(v,w) \in R^2 : \frac{\phi(v+w)}{\phi(v)} \le 1\} \tag{71}$$

Correspondingly,

$$\min\{1, \frac{\phi(v+w)}{\phi(v)}\}\phi(v) = \begin{cases} \phi(v) & \text{on } D_1 \\ \phi(v+w) & \text{on } D_2 \end{cases} \tag{72}$$

Note that $\phi(v+w)/\phi(v) = \exp[-w(w+2v)/2]$ and so

$$D_1 = \{(v,w) \in R^2 : w(w+2v) > 0\} \qquad D_2 = \{(v,w) \in R^2 : w(w+2v) \le 0\} \tag{73}$$

These domains are shown in Figure 6. With the help of this figure the integrals over D_1 and D_2 are determined in individual cases.

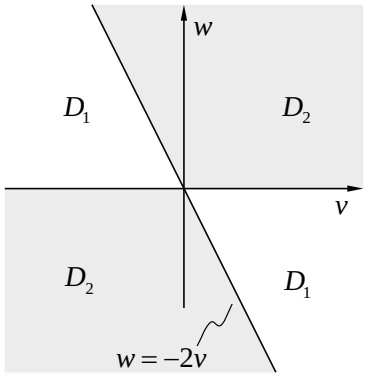

Figure 6. Integration domain D_1 and D_2

For $E[JW]$, the integral over D_1 is given by

$$\begin{aligned}
&\iint_{D_1} \min\{1, \frac{\phi(v+w)}{\phi(v)}\} w\phi(v) p^*(w) dvdw \\
&= \int_{-\infty}^{0} wp^*(w) \int_{-w/2}^{\infty} \phi(v) dvdw + \int_{0}^{\infty} wp^*(w) \int_{-\infty}^{-w/2} \phi(v) dvdw \\
&= \int_{-\infty}^{0} wp^*(w) \Phi(w/2) dw + \int_{0}^{\infty} wp^*(w) \Phi(-w/2) dw \\
&= 0
\end{aligned} \tag{74}$$

Similarly, the integral over D_2 is given by

$$\begin{aligned}
&\iint_{D_2} \min\{1, \frac{\phi(v+w)}{\phi(v)}\} w\phi(v) p^*(w) dvdw \\
&= \int_{-\infty}^{0} wp^*(w) \int_{-\infty}^{-w/2} \phi(v+w) dvdw + \int_{0}^{\infty} wp^*(w) \int_{-w/2}^{\infty} \phi(v+w) dvdw \\
&= \int_{-\infty}^{0} wp^*(w) \int_{-\infty}^{w/2} \phi(v) dvdw + \int_{0}^{\infty} wp^*(w) \int_{w/2}^{\infty} \phi(v) dvdw \\
&= \int_{-\infty}^{0} wp^*(w) \Phi(w/2) dw + \int_{0}^{\infty} wp^*(w) \Phi(-w/2) dw \\
&= 0
\end{aligned} \tag{75}$$

Combining the integral over D_1 and D_2 we conclude that

$$E[JW] = 0 \tag{76}$$

For $E[JWV]$, following similar steps gives

$$\iint_{D_1} \min\{1, \frac{\phi(v+w)}{\phi(v)}\} wv\phi(v) p^*(w) dvdw = -2\int_{0}^{\infty} wp^*(w) \phi(w/2) dw \tag{77}$$

$$\begin{aligned}
&\iint_{D_2} \min\{1, \frac{\phi(v+w)}{\phi(v)}\} wv\phi(v) p^*(w) dvdw \\
&= 2\int_{0}^{\infty} wp^*(w) \phi(w/2) dw - 2\int_{0}^{\infty} w^2 p^*(w) \Phi(-w/2) dw
\end{aligned} \tag{78}$$

Combining (77) and (78) gives,

$$E[JWV] = -2\int_{0}^{\infty} w^2 p^*(w) \Phi(-w/2) dw = -2\kappa \tag{79}$$

where $\kappa = \int_{0}^{\infty} w^2 p^*(w) \Phi(-w/2) dw$ as defined in (11).

For $E[JW^2]$, following similar steps gives

$$\iint_{D_1} \min\{1, \frac{\phi(v+w)}{\phi(v)}\} w^2\phi(v) p^*(w) dvdw = 2\int_{0}^{\infty} w^2 p^*(w) \Phi(-w/2) dw = 2\kappa \tag{80}$$

$$\iint_{D_2} \min\{1, \frac{\phi(v+w)}{\phi(v)}\} w\phi(v) p^*(w) dvdw = 2\int_{0}^{\infty} w^2 p^*(w) \Phi(-w/2) dw = 2\kappa \tag{81}$$

788 Substituting (80) and (81) into (61) gives

789 $$E[JW^2] = 4\kappa \tag{82}$$

790

791 **10. Appendix. Lower and upper bound for κ**

792 This appendix shows that $\kappa = \int_0^\infty w^2 p^*(w)\Phi(-w/2)dw$ defined in (11) is bounded

793 between 0 and 1. Let $P^*(w) = \int_{-\infty}^{w} p^*(z)dz$ be the CDF corresponding to p^*. Clearly,

794 $\kappa \geq 0$. To show $\kappa \leq 1$, integrating by parts gives

795 $$\kappa = \int_0^\infty w^2\Phi(-w/2)dP^*(w) = \frac{1}{2}\int_0^\infty P^*(w)w^2\phi(w/2)dw - 2\int_0^\infty P^*(w)w\Phi(-w/2)]dw \tag{83}$$

796 The two integrals on the RHS are non-negative. Overestimating the first with $P^*(w) \leq 1$

797 and underestimating the second with $P^*(w) \geq 1/2$ (since $w > 0$ and $p^*(w)$ is symmetric

798 about 0),

799 $$\kappa \leq \frac{1}{2}\int_0^\infty w^2\phi(w/2)dw - \int_0^\infty w\Phi(-w/2)dw \tag{84}$$

800 Integrating by parts, the second integral becomes

801 $$\int_0^\infty w\Phi(-w/2)dw = \int_0^\infty \Phi(-w/2)d(w^2/2) = \frac{1}{4}\int_0^\infty w^2\phi(w/2)dw \tag{85}$$

802 Substituting into (84) gives

803 $$\kappa \leq \frac{1}{4}\int_0^\infty w^2\phi(w/2)dw = \frac{1}{4}\int_0^\infty 8w^2\phi(w)dw = \int_{-\infty}^\infty w^2\phi(w)dw = 1 \tag{86}$$

804

805